



TECHNICAL INFORMATION

YOUNG'S MODULUS AND THERMAL DIFFUSIVITY MEASUREMENTS OF BARIUM TITANATE BASED DIELECTRIC CERAMICS

G. S. White and C. Nguyen
National Bureau of Standards
Gaithersburg, MD 20899

Bharat Rawal
AVX Corporation
Myrtle Beach, SC 29577

Abstract:

Young's modulus and thermal diffusivity values have been obtained on a set of barium titanate based ceramics using ultrasonic pulse-echo and photoacoustic effect (PAE) measurements. The PAE was shown to detect variations in thermal diffusivity between materials of varying composition and processing treatments. The results are valuable in the evaluation of dielectric ceramic materials for practical electronics applications.

YOUNG'S MODULUS AND THERMAL DIFFUSIVITY MEASUREMENTS OF BARIUM TITANATE BASED DIELECTRIC CERAMICS

G. S. White and C. Nguyen
National Bureau of Standards
Gaithersburg, MD 20899

Bharat Rawal
AVX Corporation
Myrtle Beach, SC 29577

Introduction

The use of multilayer ceramic capacitors (MLCs) is rapidly increasing in surface mount applications and, therefore, the understanding of mechanical properties and thermal shock resistance parameters of these materials is becoming increasingly important. Of the various soldering techniques utilized in surface mount applications, including wave soldering, vapor phase soldering and infrared reflow techniques, wave soldering imposes the most severe thermal stresses on the materials^{1, 2} since it involves rapid surface heat transfer from the molten metal to the terminations of the MLCs. The rapid heat transfer in processes like wave soldering results in large temperature gradients and the resulting stresses in the capacitors are further complicated by differences in the coefficients of thermal expansion and thermal diffusivities between the capacitors and other materials used in the surface mount manufacturing processes. Temperature gradients may lead to crack initiation and/or crack propagation which in turn may contribute to the subsequent deterioration of the insulation resistance of capacitors. Because barium titanate materials are often used as the major components of MLC's, there is considerable interest in the determination of the initial flaw sources and distribution, in the elastic and thermal properties, and in mechanisms by which these flaws initiate and propagate in barium titanate based dielectric materials. This work reports the results of nondestructive evaluation (NDE) measurement techniques of the Young's modulus and thermal diffusivity of several BaTiO₃ based dielectric ceramics.

Experimental Procedure

Specimens were prepared by using standard capacitor manufacturing techniques³ using the tape cast process with various dielectric compositions classified by the Electronic Industry Association (EIA) temperature characteristics referred to as X7R and Z5U ceramics. Specimens with dimensions of 25 x 25 x 3.0 mm were designated as X7R-1, X7R-2, Z5U-1, Z5U-3, and Z5U-3nb where X7R-1 and -2 are barium-bismuth titanate based dielectrics containing different minor constituents, Z5U-1 is a barium titanate-calcium zirconate based ceramic, and Z5U-3 and Z5U-3nb are relaxor based ceramic materials which are similar in composition but are processed differently.

Young's moduli (E) for the specimens were obtained using standard ultrasonic pulse-echo measurements. Measurements were made at 10 MHz, and, for both longitudinal and shear wave velocities, data were taken for

1, 2, and 3 transit times of the specimen. Uncertainty in the velocity measurements was $\leq 1.5\%$ and in the specimen density was $\leq 1\%$. Therefore, the uncertainty in E was $\leq 2.5\%$.

Values for the thermal diffusivities were obtained using the photoacoustic effect (PAE) technique following Pessoa *et al.*⁴ All specimens first were ground on both sides by a 600-grit diamond wheel to a final thickness of 0.59 mm. For purposes of comparison, the thermal diffusivity of an alumina specimen (0.64 mm thick) was also measured. Photoacoustic measurements were made using the apparatus shown in Fig. 1.

Specimens were mounted in aluminum PAE cell with a thin layer of vacuum grease as the bonding medium. Modulated radiation from a CO₂ laser, operated at 600 mW, was directed either to the front of the specimen (inside the chamber) through a ZnSe window or to the rear of the specimen through a 6 x 8 mm rectangular hole in the rear of the chamber. Laser beam modulation was achieved through the use of a mechanical chopper and frequencies ranged from 0.87 Hz to 100 Hz. The PAE signal detected by the microphone was filtered by a vector lock-in amplifier, from which phase

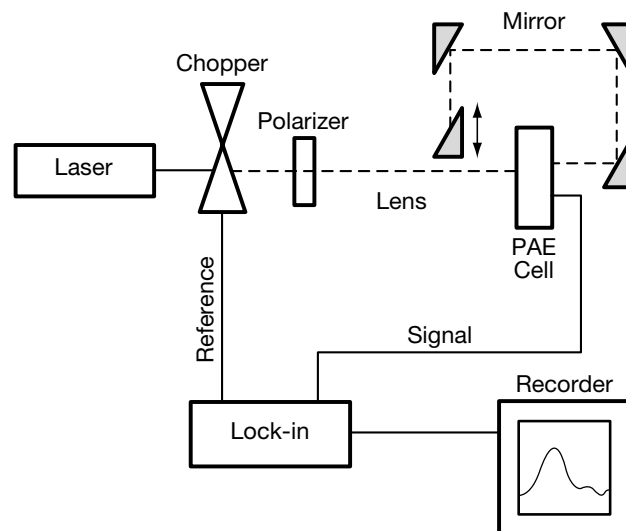


Figure 1. Schematic of photoacoustic apparatus. A mirror could be inserted or retracted to direct the modulated heating beam through the ZnSe window at the front or through a hole blocked by the specimen at the rear of the photoacoustic cell.

measurements of the signals resulting from front and rear surface heating were obtained. The frequency was monitored by an independent meter.

The PAE parameter of interest was the phase difference between front surface and rear surface heating obtained as a function of heating frequency. For some maximum frequency, f_m , the phase difference would become independent of frequency. At higher frequencies, $f > f_m$, the modulated thermal signal was unable to penetrate the specimen. Because f_m depended on the thermal properties of the particular specimen, it was not possible to predict its value precisely. Therefore, the upper limit of 100 Hz was arbitrarily chosen since it was expected that $100 \text{ Hz} \gg f_m$. The lower frequency limit, 0.87 Hz, was at the limit of the frequency response of the apparatus.

Results and Discussion

Young's Modulus Table I shows the values for the Young's moduli obtained for the five specimens:

TABLE I

Specimen	Density g/cc	Young's Modulus GPa	Thermal Diffusivity ($\times 10^{-3} \text{ cm}^2/\text{s}$)
X7R-1	5.875	148.0	5.63
X7R-2	5.834	105.0	12.35
Z5U-1	5.669	143.2	8.92
Z5U-3	8.095	131.2	4.88
Z5U-3nb	7.650	112.1	4.95

These values vary from 105.1 GPa for the X7R-2 specimen to 148.0 GPa for the X7R-1 specimen. While part of this change can be explained by changes in the compositions of the specimens, e.g., the change from 148 GPa for X7R-1 to 112.1 GPa for Z5U-3nb, some of the variation in Young's modulus must result from processing conditions, as shown by the fact that, although the Z5U-3 and the Z5U-3nb specimens are compositionally the same, E changes from 131.2 GPa for the former to 112.1 GPa for the latter. The change in the E values for the Z5U-3 and Z5U-3nb specimens reflects the fact that E is a function of the density, ρ , as well as of the longitudinal and shear wave velocities of the materials. All three of these physical parameters can vary from different processing conditions.

Because the Young's modulus is the measure of the change in stress in a material resulting from a given change in strain, it is reasonable to expect that the probability of mechanical failure resulting from thermal shock would increase with increasing E. This is certainly true for some geometries, in which the thermal stresses are proportional to E^5 .

Thermal Diffusivity The thermal diffusivities (α) of the specimens, as determined by using front and back heating in the PAE, have also been obtained and are shown in Table I. α is related to the difference in the phases of the PAE signal for front and rear surface heating, $\Delta\phi$, by the following expressions:

$$\alpha = \omega / (2a^2) = k / (\rho C)$$

$$\tan(\Delta\phi) = \tanh(al)\tan(al) \quad (1)$$

where ω is the angular modulation frequency of the heating beam, l is the specimen thickness, a is defined by eqn. 1 and is the inverse of the thermal diffusion length, k is the thermal conductivity, and C is the heat

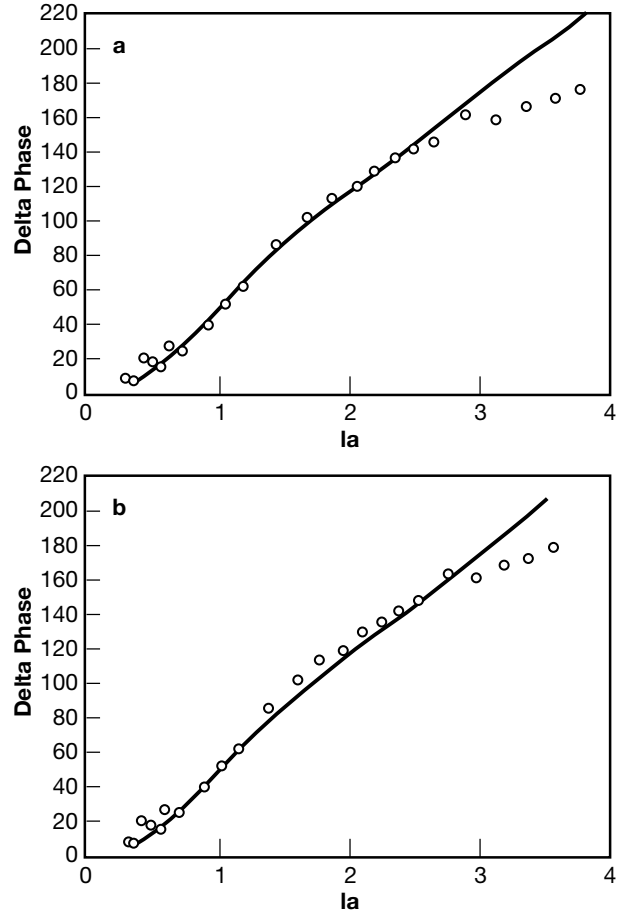


Figure 2. Plots of calculated and measured values of $\Delta\phi$ vs la for a dense Al_2O_3 specimen. a) Solid line calculated assuming $\alpha = .087 \text{ cm}^2/\text{s}$. b) Solid line calculated assuming $\alpha = .094 \text{ cm}^2/\text{s}$. Deviation of calculated values from measured values of $\Delta\phi$ begins at $la \approx 2.8$.

capacity of the specimens. To evaluate α , the experimentally obtained values of $\Delta\phi$ and the calculated values, $\tan^{-1}(\tanh(la)\tan(la))$, were plotted as functions of la . Because $la = l(\omega/(2\alpha))^{1/2}$, estimates of α were adjusted to obtain the best agreement between the measured and calculated values of $\Delta\phi$. Figure 2a is a plot of $\Delta\phi$ vs la for the alumina specimen, which was used to evaluate the accuracy of the technique for the determination of α . The symbols in the figure represent the experimental values and the solid line is calculated from eqn. 1 resulting in a value $\alpha = 0.087 \text{ cm}^2/\text{s}$. This value of α is in agreement with the literature values⁶ of α calculated from the thermal conductivity, K , specific heat, C , and density, ρ . To show the sensitivity of eqn. 1 to α . Figure 2b is a plot of the same experimental data but, this time, the solid line corresponds to $\alpha = 0.096 \text{ cm}^2/\text{s}$, a change of 10% from the previous value. The curve in Fig. 2a fits the data better than the curve in Fig. 2b, showing that eqn. 1 can determine values of α within at least 10%.

Both Figs. 2a and 2b show a deviation of the data from the calculated line for higher values of la (i.e., for modulation frequencies $> f_m$). As mentioned previously, this deviation derives from the thermal thickness of the specimen being greater than the propagation distance of the modulated heat flow, at least within the sensitivity of the experimental apparatus.

Specifically, for an alumina specimen 0.64 mm thick, with $\alpha = 0.087 \text{ cm}^2/\text{s}$, the measured values of $\Delta\phi$ deviate from the calculated values and, in fact, become constant,

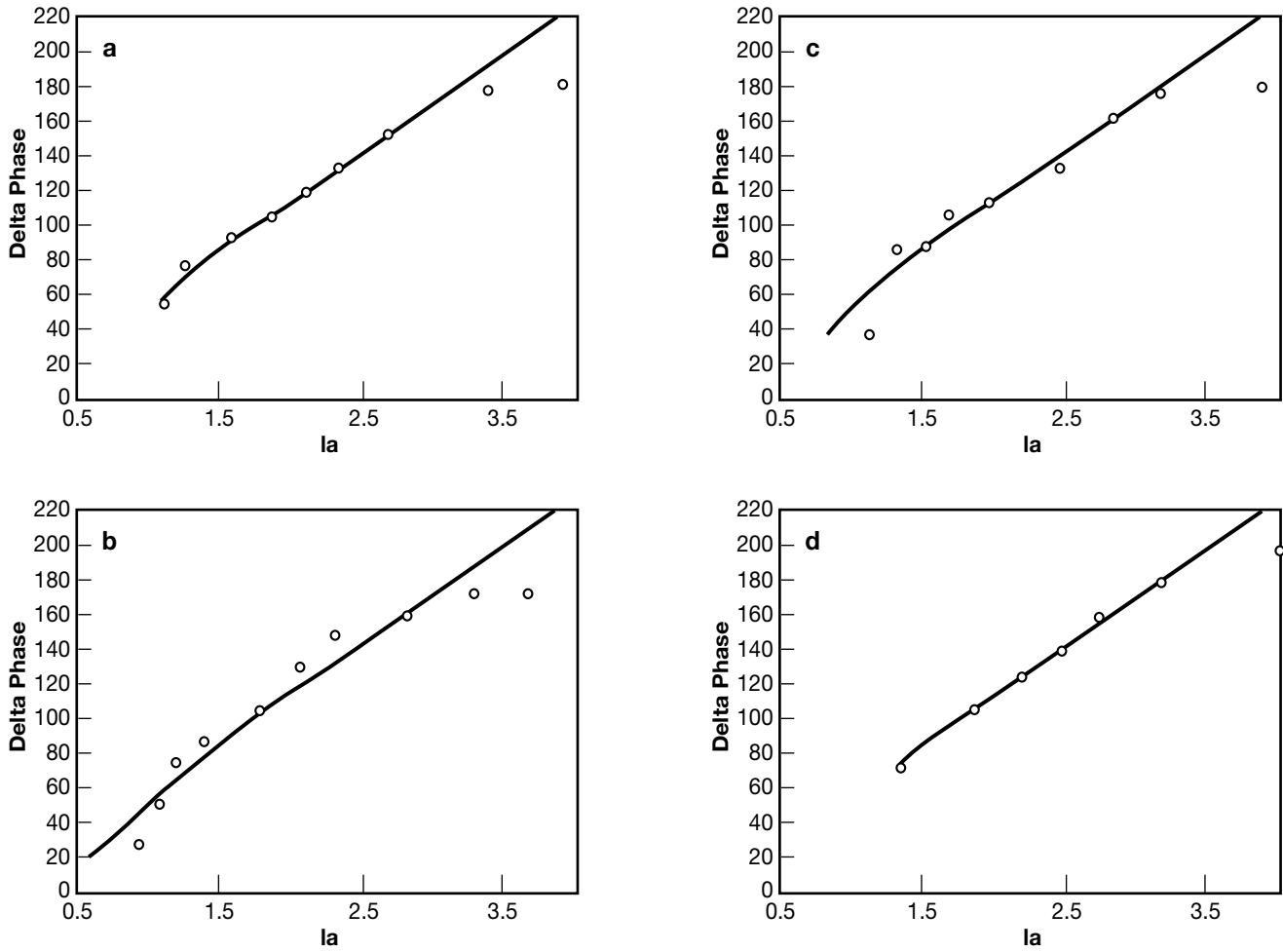


Figure 3. Calculated and measured values of $\Delta\phi$ plotted vs la for a) X7R-1, b) X7R-2, c) Z5U-1, and d) Z5U-3 specimens. Figure shows that data for all specimens begin deviating from calculated values at $la \approx 2.8$. At lower values of la , there is agreement between experimental and calculated values of $\Delta\phi$.

for $la \geq 2.8$. It must be borne in mind, however, that the value of la at which $\Delta\phi$ levels off results only from a limit in the sensitivity of the experimental apparatus, not from a change in the physical processes giving rise to the signal and, in addition, this value of la is not dependent upon the thermal properties of the specimens.

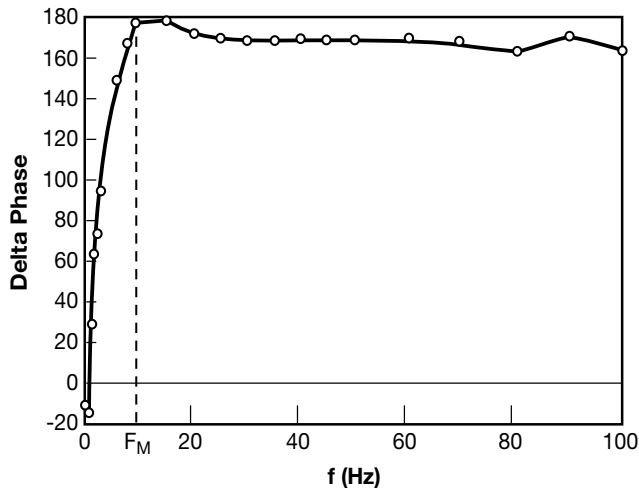


Figure 4. $\Delta\phi$ vs frequency for Z5U-1 specimen showing that $\Delta\phi$ levels off to essentially a constant value for $f \geq 9$ Hz.

Because the upper limit of la for which measurements can be made depends only on the sensitivity of the detection apparatus, it should be the same for all materials. This is shown in Fig. 3(a-d) which gives both experimental and calculated values of $\Delta\phi$ for X7R-1, X7R-2, Z5U-1 and Z5U-3. In all cases, the calculated values deviate from the experimentally obtained values at $la \approx 2.8$. This result implies that a second method of determining α is to plot $\Delta\phi$ vs f , where f is the heating modulation frequency (Fig. 4). At the frequency, f_M , at which $\Delta\phi$ becomes independent of f ,

$$\alpha \approx (1/2.8)^2 (f_M \pi). \quad (2)$$

The value 2.8 is an experimental parameter, of course, and must be determined for each PAE system. Table II lists the values and uncertainties of α determined by the two methods:

TABLE II
THERMAL DIFFUSIVITY ($\times 10^{-3}$ cm²/s)

Specimen	$\alpha_{\text{eqn 1}}$	\pm	$\alpha_{\text{eqn 2}}$	\pm
X7R-1	5.63	0.65	7.0	1.1
X7R-2	12.35	1.22	15.5	2.5
Z5U-1	8.92	1.93	9.1	4.9
Z5U-3	4.88	0.55	8.4	0
Z5U-3nb	4.95	0.73	6.7	2.5

The results shown in the Table indicate that α varies by more than a factor of two among the different materials. In particular, the thermal diffusivities of X7R-1 and X7R-2 change from 5.63 cm²/s to 12.35 cm²/s and a similar change occurs for Z5U-1 and Z5U-3. Interestingly, there is no meaningful change in α between Z5U-3 and Z5U-3nb, as determined by fitting the data to the expression in eqn. 1. Another feature shown by Table II is that the uncertainties which result from calculating α using the deviation of $\Delta\phi$ from a constant value are much larger than those obtained using eqn. 1. The increase in the uncertainty of α results from the finite number and spacing of the experimental values of the frequency. This problem is aggravated by the low thermal diffusivities of the materials under investigation. Even though the specimens were machined to ≈ 600 μm in thickness, the frequencies which would allow the thermal waves to penetrate the specimen were below 15 Hz. Since α , determined by the deviation of $\Delta\phi$ from a constant value, is directly proportional to the frequency at which the deviation occurs (eqn. 2), even a 1 Hz change in determining f_m would correspond to a 7% change in α . For the X7R-1, Z5U-3, and Z5U-3nb specimens, the upper frequency limit was even lower, resulting in larger changes in α for a 1 Hz change in f_m . In comparison, eqn. 1 allows much finer determinations of α because an entire range of data points is being used to fit the calculated curve. Therefore, although the data are restricted to the same frequency range, a change in the value of the phase measured at f_m will have much less effect on the determination of α . Therefore, while evaluating α by eqn. 2 is straight forward and provides reasonable approximations of α , fitting the data to eqn. 1 results in more accurate values of α with less uncertainty.

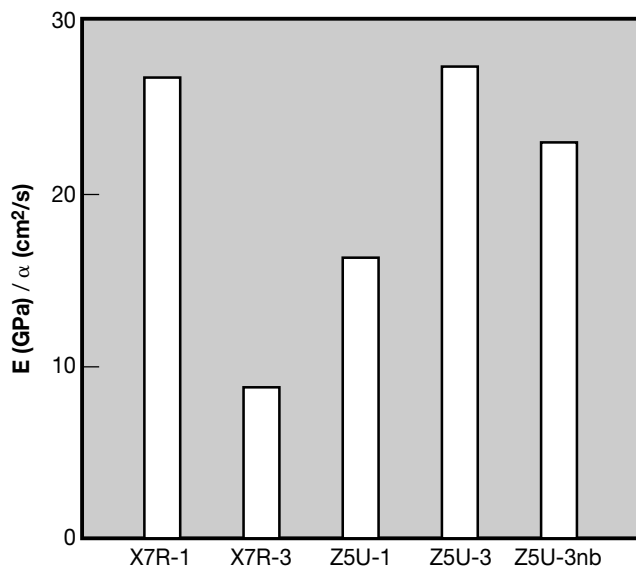


Figure 5. Values of thermal diffusivity for the 5 specimens which were investigated. The figure shows the range of values obtained in separate series of experiments.

Behavior of these materials under thermal stress

For rectangular geometries, it has been shown⁵ that the thermal stresses in the materials will increase with increasing values of E and with decreasing values of α . Figure 5 is a plot of E/α for the five materials. The larger the E/α ratio, the more susceptible the material should be to thermal shock, provided that other parameters like coefficient of thermal expansion are similar. A study of the thermal susceptibility of the capacitor chips manufactured² from these materials in fact demonstrates that X7R-1 is more susceptible to thermal shock compared to X7R-2; however, similar results were not obtained when Z5U-1 and Z5U-3 were compared because the coefficients of thermal expansion were significantly different.

Conclusions

Thermal and ultrasonic waves have been used to measure thermal diffusivities and Young's moduli in a set of barium titanate based and relaxor dielectric materials and these measurements have been used to clarify the behavior of these materials under thermal stress applications.

Acknowledgements

We would like to thank the Office of Nondestructive Evaluation at the NBS, the Office of Naval Research, and the AVX Corporation for their support of this work. We also thank E. Krasicka for assistance in setting up the ultrasound experiments.

References

1. J. Maxwell, "Surface Mount Soldering Techniques and Thermal Shock in Multilayer Ceramic Capacitors," AVX Technical Information Series (1987) 4 pp.
2. B. Rawal, R. Ladew, and R. Garcia, "Factors Responsible for Thermal Shock Behavior of Chip Capacitors," Proc. of the 37th Electronic Components Conference, Boston, MA (1987) pp. 145-156.
3. M. Kahn, "Multilayer Ceramic Capacitors - Materials and Manufacture," AVX Technical Information Series (1981) 5 pp.
4. O. Pessoa, Jr., C.L. Cesar, N.A. Patel, H. Vargas, C.C. Ghizoni and L.C.M. Miranda, "Two Beam Photoacoustic Phase Measurement of the Thermal Diffusivity of Solids," J. Appl. Phys. 59 (4), (15 Feb. 1986) pp. 1316-1318.
5. W.D. Kingery, H.K. Bowen and D.R. Uhlmann, *Introduction to Ceramics*, 2nd Edition, John Wiley and Sons, New York (1976) p. 820.
6. *Coors Alumina and Beryllia Properties Handbook*, Bulletin 952, Coors Porcelain Company, Golden, CO (1969) pp. 6-7.

USA

AVX Myrtle Beach, SC Corporate Offices

Tel: 843-448-9411
FAX: 843-626-5292

AVX Northwest, WA

Tel: 360-699-8746
FAX: 360-699-8751

AVX North Central, IN

Tel: 317-848-7153
FAX: 317-844-9314

AVX Mid/Pacific, MN

Tel: 952-974-9155
FAX: 952-974-9179

AVX Southwest, AZ

Tel: 480-539-1496
FAX: 480-539-1501

AVX South Central, TX

Tel: 972-669-1223
FAX: 972-669-2090

AVX Southeast, NC

Tel: 919-878-6223
FAX: 919-878-6462

AVX Canada

Tel: 905-564-8959
FAX: 905-564-9728

EUROPE

AVX Limited, England European Headquarters

Tel: ++44 (0) 1252 770000
FAX: ++44 (0) 1252 770001

AVX S.A., France

Tel: ++33 (1) 69.18.46.00
FAX: ++33 (1) 69.28.73.87

AVX GmbH, Germany - AVX

Tel: ++49 (0) 8131 9004-0
FAX: ++49 (0) 8131 9004-44

AVX GmbH, Germany - Elco

Tel: ++49 (0) 2741 2990
FAX: ++49 (0) 2741 299133

AVX srl, Italy

Tel: ++390 (0)2 614571
FAX: ++390 (0)2 614 2576

AVX Czech Republic, s.r.o.

Tel: ++420 (0)467 558340
FAX: ++420 (0)467 558345

ASIA-PACIFIC

AVX/Kyocera, Singapore Asia-Pacific Headquarters

Tel: (65) 258-2833
FAX: (65) 350-4880

AVX/Kyocera, Hong Kong

Tel: (852) 2-363-3303
FAX: (852) 2-765-8185

AVX/Kyocera, Korea

Tel: (82) 2-785-6504
FAX: (82) 2-784-5411

AVX/Kyocera, Taiwan

Tel: (886) 2-2696-4636
FAX: (886) 2-2696-4237

AVX/Kyocera, China

Tel: (86) 21-6249-0314-16
FAX: (86) 21-6249-0313

AVX/Kyocera, Malaysia

Tel: (60) 4-228-1190
FAX: (60) 4-228-1196

Elco, Japan

Tel: 045-943-2906/7
FAX: 045-943-2910

Kyocera, Japan - AVX

Tel: (81) 75-604-3426
FAX: (81) 75-604-3425

Kyocera, Japan - KDP

Tel: (81) 75-604-3424
FAX: (81) 75-604-3425

Contact:

NOTICE: Specifications are subject to change without notice. Contact your nearest AVX Sales Office for the latest specifications. All statements, information and data given herein are believed to be accurate and reliable, but are presented without guarantee, warranty, or responsibility of any kind, expressed or implied. Statements or suggestions concerning possible use of our products are made without representation or warranty that any such use is free of patent infringement and are not recommendations to infringe any patent. The user should not assume that all safety measures are indicated or that other measures may not be required. Specifications are typical and may not apply to all applications.

© AVX Corporation



<http://www.avxcorp.com>

S-YTMB00M900-R